Dirhodium Coordination Polymers for Asymmetric Cyclopropanation of Diazooxindoles with Olefins: Synthesis and Spectroscopic Analysis

Zhenzhong Li,[a] Lorenz Rösler,[a] Kevin Herr,[a] Martin Brodrecht,[a] Hergen Breitzke,[a] Kathrin Hofmann,[a] Hans-Heinrich Limbach,[b] Torsten Gutmann,*[a, c] and Gerd Buntkowsky*[a]

A facile approach is reported for the preparation of dirhodium coordination polymers $[Rh_2(L1)_2]_n$ (Rh_2-L1) and $[Rh_2(L2)_2]_n$ (Rh_2-L2; L1 = *N,N'*-(pyromellitoyl)-*bis*-*L*-phenylalanine diacid anion, L2 = *bis*-*N,N'*-(*L*-phenylalanyl) naphthalene-1,4,5,8-tetracarboxylate diimide) from chiral dicarboxylic acids by ligand exchange. Multiple techniques including FTIR, XPS, and $^{1}H \rightarrow {}^{13}C$ CP MAS NMR spectroscopy reveal the formation of the coordination polymers. ^{19}F MAS NMR was utilized to investigate the remaining TFA groups in the obtained coordination polymers, and demonstrated near-quantitative ligand exchange. DR-UV-vis and XPS confirm the oxidation state of the Rh center and that the Rh-single bond in the dirhodium node is maintained in the synthesis of Rh_2-L1 and Rh_2-L2. Both coordination polymers exhibit excellent catalytic performance in the asymmetric cyclopropanation reaction between styrene and diazooxindole. The catalysts can be easily recycled and reused without significant reduction in their catalytic efficiency.

Introduction

Homogeneous chiral dirhodium (II) complexes are important organometallic catalysts that have drawn much attention for asymmetric catalysis.[1–12] In particular, chiral dirhodium (II) catalysts are highly efficient catalysts for asymmetric transformations, including C–H activation, cyclopropanation, dipolar cycloaddition, X–H insertion, and ylide formation.[13–25] Recently, they have also emerged as catalysts in C–H amination and olefin aziridination.[12,26–37] This variety of reactions makes chiral dirhodium catalysts especially attractive for synthesis of pharmaceuticals or biological active substances. For example, spiro-cyclopropyloxindole compounds can be synthesized by cyclopropanation of diazooxindoles with olefins employing chiral dirhodium catalysts.[38–39] Such spiro cyclopropyloxindoles constitute an important group of heterocycles with potential application in medical research, including the use as potent HIV inhibitor[40–42] and antitumor agent.[43–46]

Despite their high activity and selectivity, the unsatisfactory catalyst recovery and recycling of the costly manufactured chiral dirhodium catalysts is the primary limiting factor for their application in chemical industry. Thus, several approaches have been proposed to handle the catalyst recovery as reviewed by Gois and co-workers.[47] Heterogenized chiral dirhodium catalysts, which are easily separable from reaction media via filtration or can be implemented in continuous flow reactors have the potential to overcome these issues, as they preserve the expensive catalysts. Accordingly, the synthesis and heterogenization of chiral dirhodium (II) complexes is currently a very active research field. A number of strategies for the heterogenization of chiral dirhodium catalysts such as forming covalent bonds via bidentate[48–52] or axial[53–56] binding were proposed. These heterogeneous catalysts were then successfully used in various asymmetric reactions. For example, Hashimoto *et al.*[57–58] developed a novel approach for immobilizing chiral dirhodium catalysts such as Rh_2(S-PTTL)$_4$ and Rh_2(S-TFPTTL)$_4$, by ligand exchange with bidentate ligands. Subsequent copolymerization then led to solid coordination polymers. Davies *et al.*[59] described a similar approach for immobilizing Rh_2(S-DOSP)$_4$ with a ligand that can be grafted to a solid support. They also reported that the immobilization of Rh_2(S-MEPY)$_4$ by anchoring the catalyst via axial binding to cross-linked macroporous polystyrene (Argopore) resin via a benzyloxymethylpyridine linker is feasible.[54] These examples clearly illustrate that significant progress has been made in immobilizing chiral dirhodium catalysts on solid carrier materials.

[a] Z. Li, L. Rösler, K. Herr, M. Brodrecht, H. Breitzke, K. Hofmann, T. Gutmann, G. Buntkowsky
Technical University of Darmstadt
Institute of Inorganic and Physical Chemistry
Alarich-Weiss-Straße 8, 64287 Darmstadt (Germany)
E-mail: gutmann@chemie.tu-darmstadt.de
gerd.buntkowsky@chemie.tu-darmstadt.de
[b] H.-H. Limbach
Freie Universität Berlin
Institute of Chemistry and Biochemistry
Takustraße 3, 14195 Berlin (Germany)
[c] T. Gutmann
University Kassel
Institute of Chemistry and Center for Interdisciplinary Nanostructure Science and Technology,
Heinrich-Plett-Straße 40, D-34132 Kassel (Germany)

Supporting information for this article is available on the WWW under https://doi.org/10.1002/cplu.202000421

Despite these remarkable achievements, however, there still remains a need for development of novel strategies to design heterogenized chiral dirhodium (II) catalysts that do not require additional solid carrier materials that may influence the activity and selectivity of the chiral dirhodium (II) catalyst.

The formation of coordination polymers is a feasible strategy to heterogenize dirhodium catalysts (II) as demonstrated by several works.[60–65] Very recently, some of us have achieved the heterogenization of dirhodium catalysts by ligand exchange employing ditopic ligands to synthesize dirhodium coordination polymers.[66–67] The structures of these as-obtained 2D coordination polymers were determined by a combination of SEM, XRD and ^{13}C and ^{19}F solid-state NMR techniques. These novel dirhodium coordination polymers exhibited an excellent catalytic efficiency in the cyclopropanation between styrene and diazoacetate. Next to these works, a series of chiral metallic coordination polymers, such as Z_1M_1-110A,[68] $\{[Ln_2(MnLCl)_2(NO_3)_2(dmf)_6(H_2O)_2] \times H_2O\}_n$ [Ln = Pr, Nd, Sm, and Gd][69] and [Co(cpfa)(bimb)] EtOH H_2O,[70] were proposed and used as catalysts for various organic reactions. This illustrates that forming a coordination polymer is a suitable way to heterogenize chiral metal containing catalysts.

However, to the best of our knowledge the synthesis and application of chiral dirhodium (II) coordination polymers by ligand substitution has not been described so far. Thus, in the present work, we report a novel and efficient approach to synthesize chiral dirhodium coordination polymer catalysts $[Rh_2(L1)_2]_n$ and $[Rh_2(L2)_2]_n$, abbreviated as Rh_2-L1 and Rh_2-L2, using $Rh_2(TFA)_4$ and chiral dicarboxylic acids as precursors. The latter are synthesized from aromatic tetracarboxylic acids with *L*-phenylalanine. The dirhodium units in these novel catalysts are connected via *N,N′*-(pyromellitoyl)-*bis*-*L*-phenylalanine diacid (H_2L1) or *bis*-*N,N′*-(*L*-phenylalanyl) naphthalene-1,4,5,8-tetracarboxylic diimide (H_2L2) ligands, respectively, depicted in Scheme 1. The as-prepared chiral dirhodium coordination polymers are characterized by a combination of different techniques such as solid-state NMR spectroscopy, FTIR, DR-UV-vis and XPS. Their catalytic activity, selectivity, stability and reusability are studied employing the formation of spiro-cyclopropyloxindole from diazooxindole and styrene as model reaction.

Results and Discussion

Synthesis and basic characterization

The synthesis of Rh_2-L1 and Rh_2-L2 is schematically depicted in Scheme 1. The chiral ligands are synthesized starting from pyromellitic dianhydride or 1,4,5,8-naphthalene dianhydride, respectively. We chose these two anhydrides owing to their high electron affinity, excellent thermal stability and feasibility

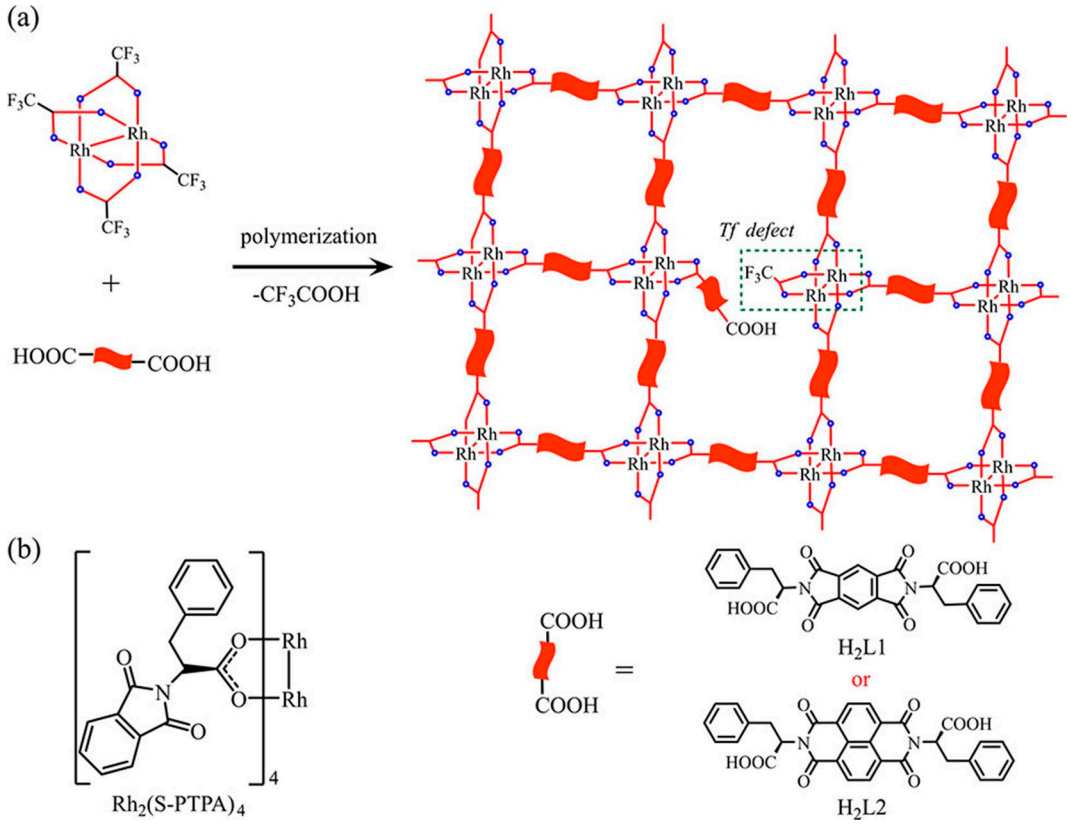

Scheme 1. (a) Synthesis of chiral dirhodium coordination polymers and possible remaining TFA containing sites. H_2L1 = *N,N′*-(pyromellitoyl)-*bis*-*L*-phenylalanine diacid, H_2L2 = *bis*-*N,N′*-(*L*-phenylalanyl) naphthalene-1,4,5,8-tetracarboxylic diimide. Note: blue circles refer to oxygen atoms. (b) Structure of the homogeneous $Rh_2(S\text{-}PTPA)_4$ catalyst.

to functionalize them through the anhydride position with arylamino or alkylamino groups.[71–73] Then, the coordination polymers were obtained by ligand exchange from the precursor $Rh_2(TFA)_4$ and H_2L1 or H_2L2, respectively (Scheme 1).

The Rh contents of the coordination polymers Rh_2-L1 and Rh_2-L2 were determined by TG analysis following the procedure of Kaskel et al.[65] (ESI Scheme S1). The nitrogen, hydrogen and carbon contents were calculated from elemental analyses. As listed in Table 1, the Rh_2 contents of catalysts Rh_2-L1 and Rh_2-L2 are 0.81 mmol and 0.76 mmol per gram catalyst, respectively. These experimental Rh_2 contents are almost equal to the predicted theoretical values 0.82 mmol and 0.75 mmol, respectively. The weight percentages (wt%) of C and N (Table 1) obtained from elemental analysis for Rh_2-L1 and Rh_2-L2 are 51.70 wt% or 55.66 wt% and 4.09 wt% or 4.33 wt%, respectively. These experimental contents show deviations from the theoretical contents especially for C (54.83 vs. 51.70 wt% and 55.66 wt% vs. 57.93 wt%). The higher theoretical values may be explained by the presence of trifluoroacetate groups in Rh_2-L1 and Rh_2-L2 that have not been substituted by chiral ligands when the coordination polymers are formed. This assumption is corroborated by the ^{19}F MAS NMR spectra of the samples (Figure 4), which display fluorine signals in Rh_2-L1 and Rh_2-L2.

A detailed analysis of these spectra is given in the section on $^{1}H \rightarrow {}^{13}C$ CP MAS and ^{19}F MAS NMR. In addition, the hydrogen contents of the samples are about 0.5 wt% higher than the theoretical values (Table 1). This is an indication of the presence of additional hydrogen sources. This hypothesis is underlined by the TG measurements of Rh_2-L1 and Rh_2-L2 (Figure S1 in the Supporting Information) that show a small decrease of mass at 100 °C. There are two probable candidates for hydrogen sources, namely the solvent ethyl acetate and water molecules.

Table 1. Compositions of Rh_2-L1 and Rh_2-L2 catalysts.

Sample	Content[a,b]	C [wt%]	H [wt%]	N [wt%]	Rh_2 [mmol/g]
Rh_2-L1	Experimental	51.70	3.538	4.09	0.81
	Theoretical	54.83	2.958	4.57	0.82
Rh_2-L2	Experimental	55.66	3.573	4.33	0.76
	Theoretical	57.93	3.039	4.22	0.75

[a] Experimental contents were determined by elemental analysis (C, H, N) or TG analysis (Rh_2). [b] Theoretical contents were calculated for the ideal framework of dirhodium units, which are connected with two chiral H_2L1 or H_2L2 groups.

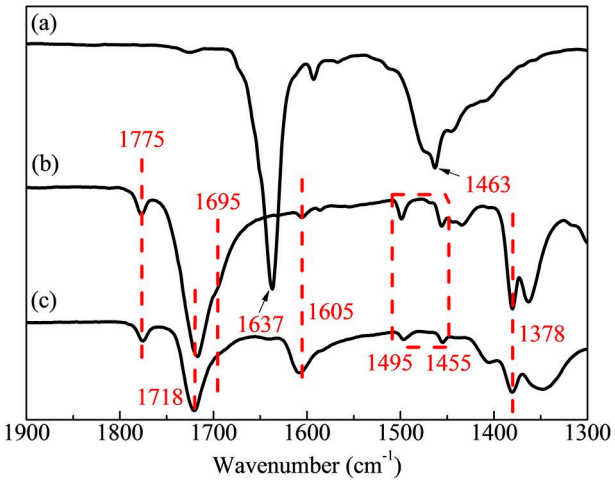

Figure 2. FT-IR spectra in the range between 1900–1300 cm^{-1} of (a) $Rh_2(TFA)_4$, (b) H_2L1 and (c) Rh_2-L1.

The morphologies of the catalysts were investigated by SEM. The SEM images in Figure 1 show that both catalysts exhibit 2D layers that are arranged as little plates/flakes in a disordered manner. Additionally, the XRD data (Figure S2 in the Supporting Information) only show very broad background signals suggesting a disordered arrangement of these layers for both catalysts.

FT-IR characterization

The FT-IR spectra of $Rh_2(TFA)_4$, H_2-L1 and Rh_2-L1 are shown in Figure 2. In the spectra of H_2L1 and Rh_2-L1 (Figure 2b, c) the signals at around 1775 and 1718 cm^{-1} are attributed to the absorption peaks of C=O asymmetric and symmetric vibration on imide moiety. The peaks around 1695 and 1605 cm^{-1} are assigned to the C=O stretching vibrations of the carboxyl/carboxylate groups of H_2L1 and Rh_2-L1.[74–75] In addition, the absorption peaks around 1495 and 1455 cm^{-1} are assigned to the breathing vibrations of C=C bonds in aromatic rings. The peak around 1378 cm^{-1} is attributed to the stretching vibrations of C–N bonds.

In the spectrum of $Rh_2(TFA)_4$ (Figure 2a), the absorption peaks at around 1637 and 1463 cm^{-1} are assigned to the C=O

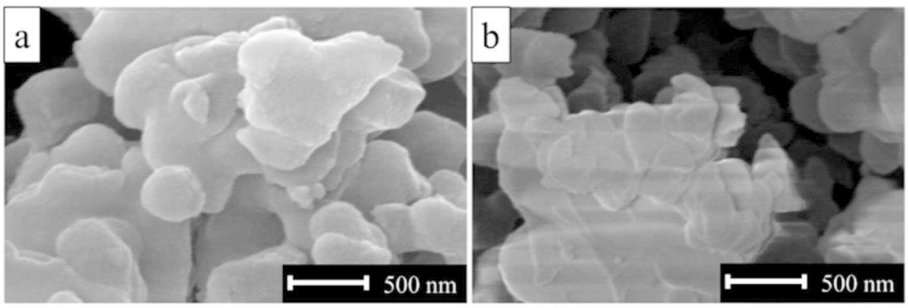

Figure 1. SEM images of (a) Rh_2-L1, (b) Rh_2-L2.

stretching vibrations of the trifluoroacetate group,[76] which have disappeared in the obtained Rh_2-L1 spectrum (Figure 2c). This is a strong indication of the success of the ligand exchange and formation of Rh_2-L1. Similar results are also obtained from the FT-IR spectra (Figure S3 in the Supporting Information) of the Rh_2-L2 catalyst.

$^{1}H\rightarrow{}^{13}C$ CP MAS and ^{19}F MAS NMR characterization

The $^{1}H\rightarrow{}^{13}C$ CP MAS NMR spectra of $Rh_2(TFA)_4$, H_2L1 and Rh_2-L1 are compared in Figure 3(I). The $^{1}H\rightarrow{}^{13}C$ CP MAS spectrum of Rh_2-L1 (Figure 3(I)c) displays three distinct resonance peaks in the range between 117 and 138 ppm, which correspond to aromatic carbons. The two small peaks around 33 and 56 ppm are assigned to the two carbon atoms C_2 and C_3 of the –N–CHR–CH_2Ph (R = –COOH) groups of the ligand system. These signals are located almost at the same position as for the ligand H_2L1 (Figure 3 Ib).

The signal around 177 ppm in the spectrum of H_2L1 (Figure 3 Ib) is characteristic for the carbon atom C_1 of carboxylate groups. This signal has disappeared and a signal at 188 ppm has appeared in the spectrum of Rh_2-L1 (Figure 3 Ic). A similar shift is obtained comparing the spectra of H_2L2 and Rh_2-L2 (Figure 3 IIb, c). Here, the peak around 177 ppm (C'_1) has disappeared and a new one at 188 ppm has appeared in the obtained spectrum of Rh_2-L2. Similar spectral changes were also reported in our previous works.[66–67]

These spectral changes strongly indicate that the carboxylate groups of H_2L*n* have displaced the trifluoroacetate groups of $Rh_2(TFA)_4$ and have coordinated with the dirhodium unit in Rh_2-L1 and Rh_2-L2.

Finally, two single peaks at around 163 and 165 ppm are visible in the spectra of H_2L1, Rh_2-L1 and H_2L2, Rh_2-L2, respectively, which most probably refer to the carbon atoms C_4 and C'_4 of imide groups.

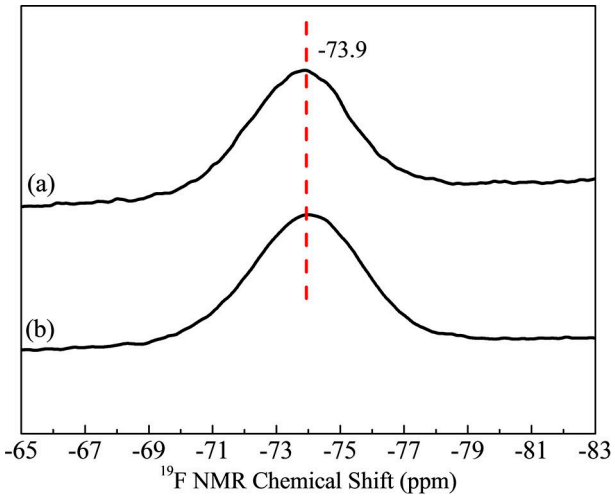

Figure 4. ^{19}F MAS NMR spectrum of (a) Rh_2-L1 and (b) Rh_2-L2.

For comparison, the $Rh_2(TFA)_4$ precursor was investigated. In Figure 3 Ia and IIa, a significant signal at 23 ppm is observed next to the signals at 178 and 111 ppm (from trifluoroacetate), which indicates acetate groups present in the $Rh_2(TFA)_4$ precursor leading to a composition of the type $Rh_2(TFA)_{4-x}(OAc)_x$. Finally, the signal at 200 ppm is assigned to COO^- of the acetate group in $Rh_2(TFA)_{4-x}(OAc)_x$.[66–67] These signals have disappeared in the spectra of Rh_2-L1 (Figure 3 Ic) and Rh_2-L2 (Figure 3 IIe).

While the results described above suggest the successful formation of the coordination polymers, they do not provide information on the quantity of the formation process. Thus, a detailed analysis of ^{19}F MAS NMR (Figure 4) spectra was

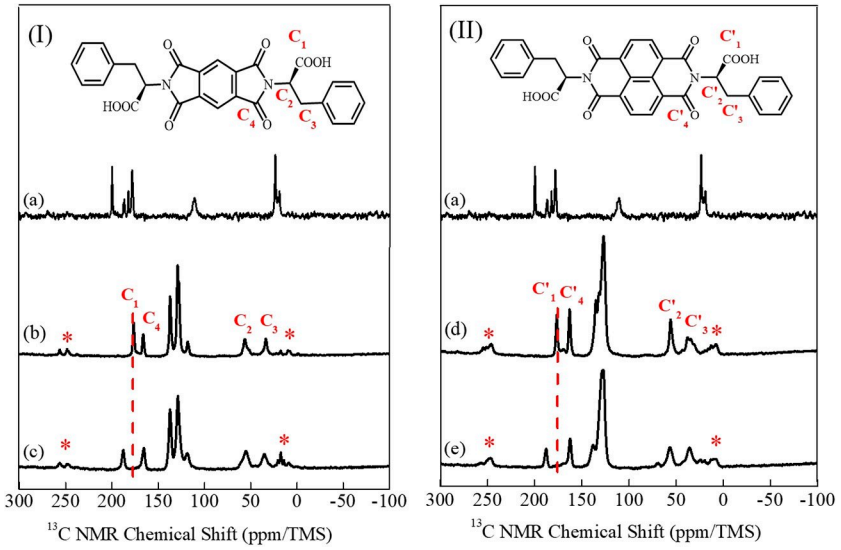

Figure 3. $^{1}H\rightarrow{}^{13}C$ CP MAS NMR spectra of (I) (a) $Rh_2(TFA)_4$, (b) H_2L1 and (c) Rh_2-L1, and (II) (a) $Rh_2(TFA)_4$, (b) H_2L2 and (c) Rh_2-L2. Note: Signals marked with * are spinning side bands of the signal at 127 ppm referring to carbon atoms in aromatic rings.

performed to provide information on the TFA containing sites occurring in the dirhodium coordination polymers. For Rh_2-L1 and Rh_2-L2, a ^{19}F signal is observed at around −73.9 ppm. This signal demonstrates the existence of trifluoroacetate groups in the dirhodium polymers. The amounts of fluorine in Rh_2-L1 and Rh_2-L2 were determined from quantitative ^{19}F MAS NMR to be 0.24 and 0.53 mmol/g, respectively (for details, see the Supporting Information). Taking the Rh_2 fraction into consideration, the Rh_2/TFA ratio for Rh_2-L1 is 10.1, while for Rh_2-L2 it is 4.2. These results demonstrate that 98% respectively 94% of the overall TFA groups are replaced during the formation process of the coordination polymers Rh_2-L1 and Rh_2-L2 (see the Supporting Information for details) and thus the exchange was almost quantitative.

DR-UV-vis and XPS

To further analyze the chemical environment in the obtained chiral dirhodium coordination polymers, diffuse reflectance ultraviolet-visible (DR-UV-vis) spectra of $Rh_2(TFA)_4$, Rh_2-L1 and Rh_2-L2 were recorded. In Figure 5, the DR-UV-vis spectra of $Rh_2(TFA)_4$ and the coordination polymers Rh_2-L1 and Rh_2-L2 are compared. All spectra display a broad band which is centered at around 450 nm (band II). In addition, a second band (band I) is obtained at different wave lengths at ca. 596, 620 or 626 nm, respectively. While band I is assigned to Rh–Rh π*→Rh–Rh σ* transitions, band II is attributed to Rh–Rh π*→Rh–O σ* transitions.[77–78] These results clearly indicate that the dirhodium unit is preserved during the synthesis of the chiral dirhodium coordination polymers. Importantly, $Rh_2(TFA)_4$ shows a significantly different position of band I compared to Rh_2-L1 and Rh_2-L2. This refers to the electronic structure of the chiral ligand systems, which is significantly different from the TFA ligand. This underlines the successful exchange of TFA ligands by the chiral ligands for both catalyst systems.

Furthermore, the electronic states of rhodium in Rh_2-L1 and Rh_2-L2 were inspected by using X-ray photoelectron spectroscopy (XPS). As illustrated in Figure 6b and c, the XPS spectra reveal that all Rh species in Rh_2-L1 and Rh_2-L2 are present in the oxidation state +2, according to the binding energies 308.3 respectively 313.2 eV of the Rh $3d_{5/2}$ and $3d_{3/2}$ levels.[78] In comparison, the parent $Rh_2(TFA)_4$ exhibits significantly different binding energies of 309.4 and 314.9 eV. Moreover, a signal around 688 eV is observed in the wide range scan of $Rh_2(TFA)_4$, which is attributed to the binding energy of F 1s. This signal has almost disappeared and a signal at 399 eV (N 1s) has appeared in the wide range scan of Rh_2-L1 and Rh_2-L2 (Figure S3 in the Supporting Information). This change of binding energies between $Rh_2(TFA)_4$ and the coordination polymers Rh_2-L1 and Rh_2-L2 further corroborates the ligand substitution and reveals that the chemical environment of the dirhodium unit is strongly affected by the chiral ligand in the dirhodium coordination polymers. Together with the FT-IR, ^{13}C CP MAS NMR and DR-UV-vis described above, these observations further confirm the success of the ligand exchange.

Catalytic tests

The catalytic performance of the Rh_2-L1 and Rh_2-L2 catalysts was tested in the asymmetric cyclopropanation reaction of diazooxindole and styrene, a model reaction to prepare spiro-cyclopropyloxindoles. Typically, in this reaction the four isomers (see scheme in Table 2) are formed, where the *R,R* and *S,S* spiro-cyclopropyloxindole (*cis*-cyclopropyloxindole) as well as *R,S* and *S,R* spiro-cyclopropyloxindole (*trans*-cyclopropyloxindole) are each pairs of enantiomers that cannot be distinguished by ^1H NMR, while *trans* and *cis*-cyclopropyloxindoles are diastereomeric to each other.

Both Rh_2-L1 and Rh_2-L2 exhibit high catalytic performance in the formation of spiro-cyclopropyloxindoles, with yields of 96% employing Rh_2-L1 and 82% for Rh_2-L2 under the same reaction conditions (0 °C, DCM as solvent, 2.5 h reaction time)

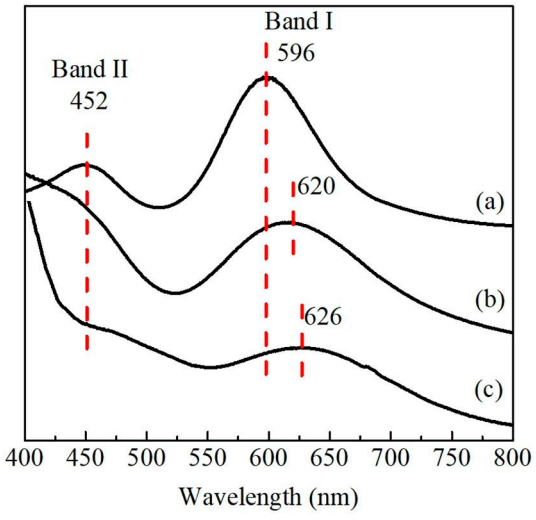

Figure 5. DR-UV-vis spectra of (a) $Rh_2(TFA)_4$, (b) Rh_2-L1 and (c) Rh_2-L2.

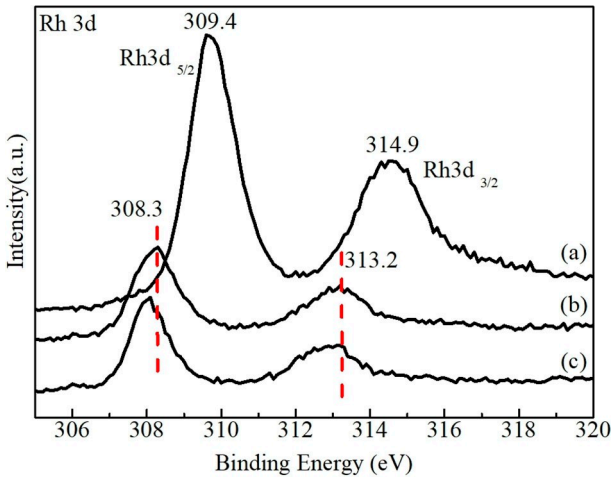

Figure 6. XPS spectra of (a) $Rh_2(TFA)_4$, (b) Rh_2-L1 and (c) Rh_2-L2.

Table 2. Asymmetric Cyclopropanation of Diazooxindole with Styrene.

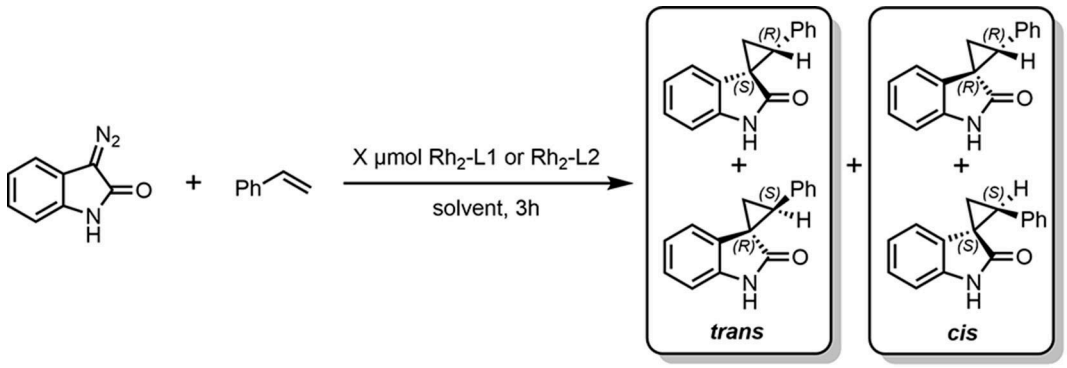

Entry	Catalyst	X [μmol]	Solvent	Temp. [°C]	[a]Yield [%]	[b]dr	[c]ee [%]
1	Rh_2-L2	3.75	DCM	0	82	83:17	7
2	Rh_2-L1	3.75	DCM	0	96	85:15	8
3	Rh_2-L1	3.75	Toluene	0	65	60:40	10
4	Rh_2-L1	3.75	DCE	0	95	88:12	13
5	Rh_2-L1	1.50	DCE	0	86	86:14	11
6	Rh_2(S-PTPA)$_4$	1.50	DCE	0	96	96:4	26

[a] Overall yields of spiro-cyclopropyloxindoles. [b] The diastereomeric ratio (*trans*:*cis*) dr was determined by ^{1}H NMR of the crude reaction mixture. [c] The [ee] was analyzed for the dominating *trans*-enantiomers. It was calculated from data determined by chiral HPLC analysis. Reaction conditions: styrene (0.75 mmol) and diazooxindole (0.15 mmol) in DCE (3 mL) were added to a two-necked round-bottom flask containing a magnetic stir bar under Ar atmosphere at 0 °C, followed by addition of the chiral dirhodium catalyst and then stirred for 3 h.

(entries 1–2). Employing an excess of the substrate styrene, as major spiro-cyclopropyloxindol products the *trans*-cyclopropyloxindole enantiomers are formed.

To identify the parameters that influence the yield and selectivity, in the next step, the reaction was performed with Rh_2-L1 as catalyst varying the solvent (DCM, toluene, DCE). This study reveals that 1,2-dichloroethane (DCE) is a more attractive solvent for this transformation in terms of both spiro-cyclopropyloxindole yield and selectivity towards the isomers.

Among the solvents tested, toluene (entry 3) has the strongest negative effect on the yield, which is significantly lowered compared to the reaction performed in DCM or DCE (entries 2, 4). The comparison of DCM with DCE shows similar yield and diastereomeric ratio, however the enantio-selectivity is lower in DCM compared to DCE (entries 2, 4).

In the next step, the influence of different amounts of catalyst is inspected. A slightly higher yield of 95% is obtained when 3.75 μmol of Rh_2-L1 is used compared to 86% when 1.50 μmol is used (entries 4–5). As expected, the diastereoselectivity and the enantioselectivity with respect to the *trans*-enantiomers are practically independent on the variation of the amount of catalyst.

Finally, the efficiencies of Rh_2-L1 and the homogeneous catalyst Rh_2(S-PTPA)$_4$ in the asymmetric cyclopropanation of styrene with diazooxindole were compared. Under similar reaction conditions, Rh_2(S-PTPA)$_4$ catalyzes the reaction to give the spiro-cyclopropyloxindoles in 96% yield with 96:4 diastereoselectivity and 26% enantioselectivity with respect to the *trans*-cyclopropyloxindole enantiomers (entry 6). In comparison with the homogeneous Rh_2(S-PTPA)$_4$, the Rh_2-L1 coordination polymer (entry 5) shows only a slightly lower diastereoselectivity and enantioselectivity.

The slightly lower yield and selectivity of the coordination polymer compared to the homogeneous catalyst may refer to different factors. (i) On the one hand, the accessibility of catalytic sites in the coordination polymer may be limited due to mass transport, which leads to a lower yield for the Rh_2-L1 coordination polymer. (ii) On the other hand, ca. 2% of trifluoroacetate groups of Rh_2(TFA)$_4$ are not exchanged by chiral ligands when the Rh_2-L1 polymer is synthesized, which yield defect sites. These defect sites are most probably responsible for the obtained selectivity of the coordination polymer. A detailed analysis whether they increase or decrease the selectivity is beyond the scope of the present work.

The obtained enantioselectivity of the investigated catalyst systems further refers to the employed ligand system. Especially, the bulkiness of the functional groups in the ligand system as well as the complexity of the ligand system itself strongly act on the enantioselectivity in cyclopropanation reactions as reviewed by Adly et al.[79] In future, to obtain higher enantioselectivity phenyl may be replaced by *tert*-butyl in the ligand system as shown by the works of Hashimoto and co-workers who applied the homogenous Rh_2(S-PTTL)$_4$ as highly enantioselective catalyst in asymmetric cyclopropanation.[80–81] Furthermore, approaches as proposed by Ball and co-workers using complex peptidic ligand systems could be included in the synthesis of coordination polymers to obtain higher selectivities.[82–83]

Recyclability and Leaching test

To test the stability and reusability of the novel dirhodium coordination polymers, the Rh_2-L1 catalyst was investigated in

an exemplary way in the asymmetric cyclopropanation reaction between diazooxindole and styrene. Typically, the catalyst was separated from the reaction system by centrifugation and washed with ethyl acetate several times to be reused in another run under the same conditions. As shown in Figure 7 no significant decrease in the yield is obtained after Rh_2-L1 was used repetitively five times. This obviously displays the excellent stability and reusability of this chiral catalyst.

Meanwhile, the diastereomeric ratio slightly drops down (ESI Table S3). The enantioselectivity with respect to the *trans*-enantiomers as well gradually drops down with increasing number of cycles (Figure 7) as has been also observed for other catalysts in the past.[78] This indicates that the chemical environment around the Rh_2 unit changed. However, the Rh_2-L1 catalyst still shows good catalytic activity as figured out by the calculated TOFs at 1.5 h and 3 h of reaction (see Table S2 in the Supporting Information), which do not significantly change with the number of reaction cycles.

Finally, the leaching level of rhodium was examined by ICP-OES analysis. The result was that any possible amounts of leached Rhodium are below the detection threshold of ICP-OES (< 0.05 ppm, see Table S4 in the Supporting Information).

Conclusion

A facile approach to prepare novel chiral dirhodium coordination polymers from the precursors $Rh_2(TFA)_4$ and chiral dicarboxylic acids via ligand exchange was developed. The coordination polymers consist of 2D layers arranged as plates/flakes in a disordered manner as demonstrated by SEM. Characterization by FT-IR, ^{13}C CP MAS NMR and XPS revealed the successful ligand exchange. Quantitative ^{19}F MAS NMR showed that the ligand exchange was nearly quantitative (> 95%). During the ligand substitution process, the dirhodium unit stayed intact as proved by DR-UV-vis and XPS.

The catalytic performance, diastereoselectivity and enantioselectivity of the coordination polymers depended on the used chiral ligand system and was only slightly reduced compared with the homogeneous catalyst, Rh_2(S-PTPA)$_4$. The coordination polymer Rh_2-L1 showed excellent stability with negligible leaching and could be easily recycled and reused at least five times without significant loss of catalytic activity. After optimization, this one-pot synthetic approach for preparation of Rh_2-L1 and Rh_2-L2 may be extended to develop chiral dirhodium coordination polymers with different chiral ligands for chemical transformations with high selectivity in future.

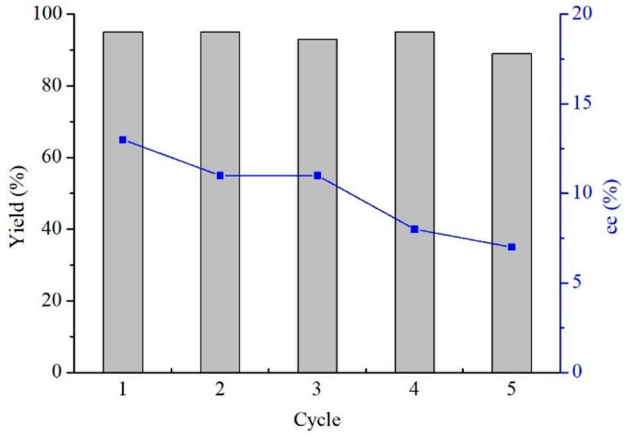

Figure 7. Recyclability test of Rh_2-L1 in the asymmetric cyclopropanation between styrene and diazooxindole.

Experimental Section

Materials

Rhodium trifluoroacetate ($Rh_2(TFA)_4$, Acros Organics), pyromellitic dianhydride (Alfa Aesar), naphthalene-1,4,5,8-tetracarboxylic acid dianhydride (Alfa Aesar), *L*-phenylalanine (Carl Roth), styrene (Sigma-Aldrich), *N,N*-dimethylformamide (Sigma-Aldrich), isatin (Acros Organics), *p*-toluenesulfonyl hydrazide ($TsNHNH_2$, Acros Organics), acetic acid (Sigma-Aldrich), dichloromethane (Sigma-Aldrich), 1,2-dichloroethane (Sigma-Aldrich), toluene (Sigma-Aldrich) and ethyl acetate 99.5% puriss. (Sigma-Aldrich) were purchased and used without further purification.

Synthesis of chiral diacid ligands

***N,N'*-(pyromellitoyl)-*bis*-*L*-phenylalanine diacid (H_2-L1):** H_2-L1 was prepared according to the procedure reported elsewhere.[75,84] A mixture of pyromellitic dianhydride (2.18 g, 10 mmol) and *L*-phenylalanine (3.30 g, 20 mmol) was dissolved in 30 mL acetic acid and stirred at room temperature for 5 h, followed by heating under reflux for 6–8 h. The solvent was removed under reduced pressure and the residue was dissolved in 50 mL of cold 1 M hydrochloric acid. The solution was stirred until a white precipitate was formed. This precipitate was filtered off, washed with 200 mL of deionized water and dried under vacuum. (4.40 g, 86% yield), ^1H NMR (300 MHz, DMSO-d_6) δ: 13.33 (s, 2H), 8.20 (s, 2H), 7.28–7.08 (m, 10H), 5.18 (dd, J = 11.3, 4.8 Hz, 2H), 3.51-3.55 (dd, J = 14.1, 4.8 Hz, 2H), 3.38–3.33 (m, 2H). ^{13}C NMR (75 MHz, DMSO-d_6) δ: 169.53, 165.14, 137.09, 136.20, 128.66, 128.32, 126.57, 118.36, 53.63, 33.90.

***Bis*-*N,N'*-(*L*-phenylalanyl) naphthalene-1,4,5,8-tetracarboxylic diimide (H_2-L2):** H_2-L2 was synthesized according to the procedure reported elsewhere.[85–86] A mixture of 1,4,5,8-naphthalene dianhydride (0.95 g, 3.56 mmol) and *L*-phenylalanine (1.18 g, 7.13 mmol) was suspended in 20 mL of *N,N*-dimethylformamide (DMF) and refluxed for 12 h, giving a brown solution. This solution was cooled to room temperature before it was poured over ice. The product was extracted with ethyl acetate (2 × 100 mL), washed with brine, and the solvent was removed under vacuum. The solid was washed with toluene to give the product. (1.39 g, 70% yield), ^1H NMR (300 MHz, DMSO-d_6) δ: 13.06 (br., 2H), 8.65 (s, 4H), 7.01–7.18 (m, 10H), 5.86 (dd, J = 9.5, 5.6 Hz, 2H), 3.60 (dd, J = 13.9, 5.6 Hz, 2H), 3.33 (dd, J = 14.2, 9.3 Hz, 2H), ^{13}C NMR (75 MHz, DMSO-d_6) δ: 170.69, 162.46,

138.26, 131.70, 129.41, 128.60, 126.80, 126.47, 125.13, 55.06, 34.78.

Synthesis of chiral dirhodium coordination polymers: The heterogeneous chiral dirhodium polymers were obtained by ligand exchange according to the literature.[66–67]

Rh_2-L1 was synthesized as follows. A solution of $Rh_2(TFA)_4$ (0.10 g, 0.15 mmol) and H_2L1 (0.23 g, 0.46 mmol) in 75 mL ethyl acetate (EtOAc) was charged into a 100 mL round-bottomed flask which was fitted with a Soxhlet extractor containing a mixture of 1 g K_2CO_3 and 1 g 4 Å molecular sieve in a cellulose filter tube. This first Soxhlet approach was used to neutralize the formed trifluoroacetic acid upon ligand exchange and shift the equilibrium towards the formation of the coordination polymer. After 3 days reaction under reflux, the obtained solid was filtered and washed in a Soxhlet extractor by EtOAc for another 2 days. This second Soxhlet step, which is performed in the absence of K_2CO_3 is a simple washing step, which is not expected to influence the constitution of the product. Then, the solid was dried at 80 °C under vacuum for 12 h yielding Rh_2-L1 (72.9 mg, 38% yield).

Rh_2-L2 was synthesized similarly, employing a mixture of $Rh_2(TFA)_4$ (0.1 g, 0.15 mmol) and H_2L2 (0.26 g, 0.46 mmol) in 75 mL EtOAc. The reaction was performed at 120 °C for 5 days yielding Rh_2-L2 (51.2 mg, 24% yield).

Catalytic Asymmetric Cyclopropanation

3-Diazooxindole was prepared according to the literature.[87] A mixture of isatin (1.47 g, 10 mmol) and $TsNHNH_2$ (2.05 g, 11 mmol) in THF (50 mL) was stirred at 65 °C for 1 h. After filtration, the solid was stirred in 50 mL of a 0.2 M NaOH aqueous solution at 65 °C for 1 h. The reaction mixture was then extracted with EtOAc (80 mL, three times). The combined organic phases were dried over Na_2SO_4 and the solvent was removed under vacuum. The residue was recrystallized from acetone to give the 3-diazooxindole as an orange solid (1.29 g, 81% yield). ^{1}H NMR (300 MHz, $CDCl_3$) δ: 9.46 (s, 1 H), 7.18-93 (m, 4 H), ^{13}C NMR (75 MHz, $CDCl_3$) δ: 169.35, 131.96, 125.56, 122.14, 118.31, 117.25, 110.78.

The catalytic cyclopropanation of styrene with diazooxindole was applied to evaluate the performance of the Rh_2-L1 and Rh_2-L2 catalysts. In detail, styrene (0.75 mmol) and diazooxindole (0.15 mmol) in 3 mL of an appropriate solvent (here we focused on dichloromethane (DCM), dichloroethane (DCE) and toluene according to refs. [38–39]) were added to a two-necked round-bottom flask equipped with a magnetic stir bar followed by addition of a specific amount (1.50 or 3.75 μmol Rh_2) of the chiral dirhodium catalyst. The reaction was performed under Ar atmosphere at 0 °C. After stirring for 3 h, the chiral dirhodium catalyst was removed by centrifugation and the solvent was removed under reduced pressure. The diastereomeric ratio (dr) was determined by crude ^{1}H NMR analysis (for details see the Supporting Information).

The resulting crude mixture was further purified by silica gel column chromatography (hexane-EtOAc = 2:1 to 1:1) to concentrate the *trans*-enantiomers for determination of the enantiomeric excess (ee). ^{1}H NMR of the *trans*-enantiomers (300 MHz, $CDCl_3$) δ: 9.09 (br, 1 H), 7.33–7.22 (m, 5 H), 7.11 (t, J = 7.7 Hz, 1 H), 6.97 (d, J = 7.5 Hz, 1 H), 6.69 (m, 1 H), 5.96 (d, J = 7.5 Hz, 1 H), 3.37 (t, J = 8.6 Hz, 1 H, *trans*), 2.28–2.23 (m,1 H), 2.08–2.05 (m, 1 H); ^{13}C NMR (75 MHz, $CDCl_3$) δ: 178.89, 141.04, 134.99, 129.95, 128.38, 127.91, 127.44, 126.58, 121.43, 120.97, 109.69, 36.14, 33.74, 22.65. The enantiomeric excess (ee) was then calculated for the *trans*-enantiomers from data determined by chiral HPLC analysis (for details see the Supporting Information).

Recyclability test

To inspect the recyclability of the coordination polymers, experiments were exemplary performed for Rh_2-L1. The catalyst was separated from the reaction mixture, washed and dried after each run of reaction. Then, the Rh_2-L1 catalyst was tested with a fresh mixture of reactants and solvent for subsequent reaction under the same conditions. Rh_2-L1 was recycled 5 times.

For the leaching test, the Rh_2-L1 catalyst was removed, the filtrated solution was collected and the residual rhodium fraction were studied with ICP-OES.

Characterization

Thermogravimetric (TG) analyses were carried out under oxygen flow (75 mL min^{-1}) using the simultaneous thermal analyzer TG 209 F3 Tarsus. The Rh loadings were calculated from the TG analysis data according to the method reported by Kaskel *et al.*[65] The C, N and H contents were determined on an Elemental Analyzer Vario EL III working in CHN mode.

Fourier-transform infrared spectroscopy (FTIR) was conducted using a Perkin Elmer Spectrum spotlight 200 FT-IR spectrometer with 4 cm^{-1} resolution.

Scanning electron microscopy (SEM) images were obtained using a Philips XL30 S-FEG microscope to probe the coordination polymers employing an electron beam energy of 20 keV.

X-ray powder diffraction (XRD) patterns were measured on a powder diffractometer (StadiP, Stoe & Cie. GmbH, Darmstadt, Germany) in transmission geometry using Cu Kα_1-radiation (λ = 154.060 pm, Ge[111]-monochromator) and a MYTHEN 1 K (Dectris Ltd. Baden, Switzerland) detector. The samples were placed between two X-ray amorphous foils and were measured in the 2θ range of 3–50°.

^{1}H→^{13}C CP MAS NMR spectra were measured at room temperature on a 9.4 T Bruker Avance II+ solid state NMR spectrometer with a 4 mm broadband double-resonance probe at a frequency of 100.61 MHz for ^{13}C. For all samples cross polarization experiments were performed with contact times of 1.5 ms at a spinning rate of 12 kHz. 20480 scans were applied with a repetition delay of 2 s. Spectra were referenced to TMS using adamantane (δ = 38.5 ppm) as external standard.

^{19}F MAS NMR spectra were measured on a 9.4 T Bruker Avance II+ solid state NMR spectrometer at a frequency of

376.50 MHz, employing a 3.2 mm double-resonance probe. All samples were measured at a spinning rate of 17 kHz. Spectra were recorded with single pulse excitation employing a 20° excitation pulse of 0.46 μs. 512 scans were applied with a repetition delay of 300 s to ensure the observation of quantitative spectra. Details on the quantitative analysis are given in the Supporting Information. Spectra were referenced to $CFCl_3$ employing solid BaF_2 ($\delta = -14.35$ ppm) as external standard.

The diffuse reflection ultraviolet-visible spectrum (DR-UV vis) was measured on a Shimadzu UV 2450 spectrophotometer using $BaSO_4$ as a reference. X-ray photoelectron spectroscopy (XPS) measurements were performed using an Electronic Versaprobe 5000 spectrometer with a monochromatic Al–Kα source at an incidence angle of 45°. The binding energy of the C1s peak at 284.8 eV was employed to reference the spectra.

Acknowledgements

This work has been supported by the DFG under contract Bu 911/27-1. Open access funding enabled and organized by Projekt DEAL.

Conflict of Interest

The authors declare no conflict of interest.

Keywords: asymmetric cyclopropanation · coordination polymers · heterogenous catalysis · ligand exchange · rhodium

[1] D. T. Boruta, O. Dmitrenko, G. P. Yap, J. M. Fox, *Chem. Sci.* **2012**, *3*, 1589–1593.
[2] H. M. Davies, A. M. Walji, *Org. Lett.* **2003**, *5*, 479–482.
[3] A. DeAngelis, O. Dmitrenko, G. P. Yap, J. M. Fox, *J. Am. Chem. Soc.* **2009**, *131*, 7230–7231.
[4] M. El-Deftar, F. G. Adly, M. G. Gardiner, A. Ghanem, *Curr. Org. Chem.* **2012**, *16*, 1808–1836.
[5] S. K. Gadakh, S. Dey, A. Sudalai, *J. Org. Chem.* **2015**, *80*, 11544–11550.
[6] Z. Li, H. M. Davies, *J. Am. Chem. Soc.* **2009**, *132*, 396–401.
[7] Y. Natori, M. Ito, M. Anada, H. Nambu, S. Hashimoto, *Tetrahedron Lett.* **2015**, *56*, 4324–4327.
[8] P. Panne, A. DeAngelis, J. M. Fox, *Org. Lett.* **2008**, *10*, 2987–2989.
[9] D. Rackl, C.-J. Yoo, C. W. Jones, H. M. Davies, *Org. Lett.* **2017**, *19*, 3055–3058.
[10] R. P. Reddy, H. M. Davies, *J. Am. Chem. Soc.* **2007**, *129*, 10312–10313.
[11] B. D. Schwartz, J. R. Denton, Y. Lian, H. M. Davies, C. M. Williams, *J. Am. Chem. Soc.* **2009**, *131*, 8329–8332.
[12] P.-A. Chen, K. Setthakarn, J. A. May, *ACS Catal.* **2017**, *7*, 6155–6161.
[13] F. G. Adly, M. G. Gardiner, A. Ghanem, *Chem. Eur. J.* **2016**, *22*, 3447–3461.
[14] H. M. Davies, R. E. Beckwith, *Chem. Rev.* **2003**, *103*, 2861–2904.
[15] H. M. Davies, J. R. Denton, *Chem. Soc. Rev.* **2009**, *38*, 3061–3071.
[16] H. M. Davies, J. R. Manning, *Nature* **2008**, *451*, 417.
[17] H. M. Davies, D. Morton, *Chem. Soc. Rev.* **2011**, *40*, 1857–1869.
[18] M. P. Doyle, R. Duffy, M. Ratnikov, L. Zhou, *Chem. Rev.* **2009**, *110*, 704–724.
[19] P. M. Gois, C. A. Afonso, *Eur. J. Org. Chem.* **2004**, *2004*, 3773–3788.
[20] D. M. Hodgson, R. Glen, A. J. Redgrave, *Tetrahedron: Asymmetry* **2009**, *20*, 754–757.
[21] T. Miyazawa, K. Minami, M. Ito, M. Anada, S. Matsunaga, S. Hashimoto, *Tetrahedron* **2016**, *72*, 3939–3947.
[22] R. P. Reddy, G. H. Lee, H. M. Davies, *Org. Lett.* **2006**, *8*, 3437–3440.
[23] H. Saito, H. Oishi, S. Kitagaki, S. Nakamura, M. Anada, S. Hashimoto, *Org. Lett.* **2002**, *4*, 3887–3890.
[24] M.-Y. Huang, J.-M. Yang, Y.-T. Zhao, S.-F. Zhu, *ACS Catal.* **2019**, *9*, 5353–5357.
[25] J. Liu, A. Plog, P. Groszewicz, L. Zhao, Y. Xu, H. Breitzke, A. Stark, R. Hoffmann, T. Gutmann, K. Zhang, *Chem. Eur. J.* **2015**, *21*, 12414–12420.
[26] R. P. Reddy, H. M. Davies, *Org. Lett.* **2006**, *8*, 5013–5016.
[27] K. W. Fiori, J. Du Bois, *J. Am. Chem. Soc.* **2007**, *129*, 562–568.
[28] C. Liang, F. Collet, F. Robert-Peillard, P. Müller, R. H. Dodd, P. Dauban, *J. Am. Chem. Soc.* **2008**, *130*, 343–350.
[29] D. N. Zalatan, J. Du Bois, *J. Am. Chem. Soc.* **2008**, *130*, 9220–9221.
[30] F. Collet, R. H. Dodd, P. Dauban, *Chem. Commun.* **2009**, 5061–5074.
[31] S. Sato, M. Shibuya, N. Kanoh, Y. Iwabuchi, *Chem. Commun.* **2009**, 6264–6266.
[32] C.-M. Che, V. K.-Y. Lo, C.-Y. Zhou, J.-S. Huang, *Chem. Soc. Rev.* **2011**, *40*, 1950–1975.
[33] J. Du Bois, *Org. Process Res. Dev.* **2011**, *15*, 758–762.
[34] J. L. Jat, M. P. Paudyal, H. Gao, Q.-L. Xu, M. Yousufuddin, D. Devarajan, D. H. Ess, L. Kürti, J. R. Falck, *Science* **2014**, *343*, 61–65.
[35] Z. Ma, Z. Zhou, L. Kürti, *Angew. Chem. Int. Ed.* **2017**, *56*, 9886–9890.
[36] M. P. Paudyal, A. M. Adebesin, S. R. Burt, D. H. Ess, Z. Ma, L. Kürti, J. R. Falck, *Science* **2016**, *353*, 1144–1147.
[37] S. Kang, H.-K. Lee, *J. Org. Chem.* **2009**, *75*, 237–240.
[38] T. Arai, A. Awata, *Synlett* **2012**, *24*, 29–32.
[39] Y. Chi, L. Qiu, X. Xu, *Org. Biomol. Chem.* **2016**, *14*, 10357–10361.
[40] T. Jiang, K. L. Kuhen, K. Wolff, H. Yin, K. Bieza, J. Caldwell, B. Bursulaya, T. Y.-H. Wu, Y. He, *Bioorg. Med. Chem. Lett.* **2006**, *16*, 2105–2108.
[41] G. Kumari, M. Modi, S. K. Gupta, R. K. Singh, *Eur. J. Med. Chem.* **2011**, *46*, 1181–1188.
[42] M. Palomba, L. Rossi, L. Sancineto, E. Tramontano, A. Corona, L. Bagnoli, C. Santi, C. Pannecouque, O. Tabarrini, F. Marini, *Org. Biomol. Chem.* **2016**, *14*, 2015–2024.
[43] P. B. Sampson, Y. Liu, N. K. Patel, M. Feher, B. Forrest, S.-W. Li, L. Edwards, R. Laufer, Y. Lang, F. Ban, *J. Med. Chem.* **2014**, *58*, 130–146.
[44] P. B. Sampson, Y. Liu, B. Forrest, G. Cumming, S.-W. Li, N. K. Patel, L. Edwards, R. Laufer, M. Feher, F. Ban, *J. Med. Chem.* **2014**, *58*, 147–169.
[45] B. Yu, Z. Yu, P.-P. Qi, D.-Q. Yu, H.-M. Liu, *Eur. J. Med. Chem.* **2015**, *95*, 35–40.
[46] C. N. Reddy, V. L. Nayak, G. S. Mani, J. S. Kapure, P. R. Adiyala, R. A. Maurya, A. Kamal, *Bioorg. Med. Chem. Lett.* **2015**, *25*, 4580–4586.
[47] N. R. Candeias, C. A. M. Afonso, P. M. P. Gois, *Org. Biomol. Chem.* **2012**, *10*, 3357–3378.
[48] M. P. Doyle, D. J. Timmons, J. S. Tumonis, H.-M. Gau, E. C. Blossey, *Organometallics* **2002**, *21*, 1747–1749.
[49] H. M. Hultman, M. de Lang, M. Nowotny, I. W. Arends, U. Hanefeld, R. A. Sheldon, T. Maschmeyer, *J. Catal.* **2003**, *217*, 264–274.
[50] M. P. Doyle, M. Yan, H.-M. Gau, E. C. Blossey, *Org. Lett.* **2003**, *5*, 561–563.
[51] L. Chen, T. Yang, H. Cui, T. Cai, L. Zhang, C.-Y. Su, *J. Mater. Chem. A* **2015**, *3*, 20201–20209.
[52] B. Zhu, G. Liu, L. Chen, L. Qiu, L. Chen, J. Zhang, L. Zhang, M. Barboiu, R. Si, C.-Y. Su, *Inorg. Chem. Front.* **2016**, *3*, 702–710.
[53] H. M. Davies, A. M. Walji, T. Nagashima, *J. Am. Chem. Soc.* **2004**, *126*, 4271–4280.
[54] H. M. Davies, A. M. Walji, *Org. Lett.* **2005**, *7*, 2941–2944.
[55] F. G. Adly, A. Ghanem, *Tetrahedron Lett.* **2016**, *57*, 852–857.
[56] A. F. Trindade, J. A. S. Coelho, C. A. M. Afonso, L. F. Veiros, P. M. P. Gois, *ACS Catal.* **2012**, *2*, 370–383.
[57] K. Takeda, T. Oohara, M. Anada, H. Nambu, S. Hashimoto, *Angew. Chem. Int. Ed.* **2010**, *49*, 6979–6983.
[58] T. Oohara, H. Nambu, M. Anada, K. Takeda, S. Hashimoto, *Adv. Synth. Catal.* **2012**, *354*, 2331–2338.
[59] K. M. Chepiga, Y. Feng, N. A. Brunelli, C. W. Jones, H. M. Davies, *Org. Lett.* **2013**, *15*, 6136–6139.
[60] S. Takamizawa, E.-I. Nakata, H. Yokoyama, K. Mochizuki, W. Mori, *Angew. Chem. Int. Ed.* **2003**, *42*, 4331–4334.
[61] Y. Kataoka, K. Sato, Y. Miyazaki, Y. Suzuki, H. Tanaka, Y. Kitagawa, T. Kawakami, M. Okumura, W. Mori, *Chem. Lett.* **2010**, *39*, 358–359.
[62] K. Arakawa, N. Yano, N. Imasaki, Y. Kohara, D. Yatsushiro, D. Atarashi, M. Handa, Y. Kataoka, *Crystals* **2020**, *10*.
[63] F. A. Cotton, E. V. Dikarev, M. A. Petrukhina, S. E. Stiriba, *Polyhedron* **2000**, *19*, 1829–1835.
[64] Y. Kataoka, N. Yano, T. Shimodaira, Y.-N. Yan, M. Yamasaki, H. Tanaka, K. Omata, T. Kawamoto, M. Handa, *Eur. J. Inorg. Chem.* **2016**, *2016*, 2810–2815.

[65] G. Nickerl, U. Stoeck, U. Burkhardt, I. Senkovska, S. Kaskel, *J. Mater. Chem. A* **2014**, *2*, 144–148.
[66] J. Liu, C. Fasel, P. Braga-Groszewicz, N. Rothermel, A. S. L. Thankamony, G. Sauer, Y. Xu, T. Gutmann, G. Buntkowsky, *Catal. Sci. Technol.* **2016**, *6*, 7830–7840.
[67] J. Liu, Y. Xu, P. B. Groszewicz, M. Brodrecht, C. Fasel, K. Hofmann, X. Tan, T. Gutmann, G. Buntkowsky, *Catal. Sci. Technol.* **2018**, *8*, 5190–5200.
[68] J. Amaro-Gahete, D. Esquivel, J. R. Ruiz, C. Jiménez-Sanchidrián, F. J. Romero-Salguero, *Appl. Catal. A* **2019**, *585*, 117190.
[69] M. Yadav, A. Bhunia, S. K. Jana, P. W. Roesky, *Inorg. Chem.* **2016**, *55*, 2701–2708.
[70] X. Xu, Y.-H. Yu, G.-F. Hou, X.-W. Li, C.-Y. Ren, D.-S. Ma, *Polyhedron* **2016**, *112*, 61–66.
[71] C. Huang, S. Barlow, S. R. Marder, *J. Org. Chem.* **2011**, *76*, 2386–2407.
[72] F. Würthner, M. Stolte, *Chem. Commun.* **2011**, *47*, 5109–5115.
[73] M. Al Kobaisi, S. V. Bhosale, K. Latham, A. M. Raynor, S. V. Bhosale, *Chem. Rev.* **2016**, *116*, 11685–11796.
[74] S. Mallakpour, H. Ayatollahi, *J. Thermoplast. Compos. Mater.* **2015**, *28*, 3–18.
[75] P. Li, F. He, Z. Yang, W. Yang, J. Yao, *Polym. Degrad. Stab.* **2018**, *147*, 267–273.
[76] G. Winkhaus, P. Ziegler, *Z. Anorg. Allg. Chem.* **1967**, *350*, 51–61.
[77] K. Sanada, H. Ube, M. Shionoya, *J. Am. Chem. Soc.* **2016**, *138*, 2945–2948.
[78] E. B. Boyar, S. D. Robinson, *Coord. Chem. Rev.* **1983**, *50*, 109–208.
[79] F. G. Adly, *Catalysts* **2017**, *7*, 347.
[80] K. Minami, H. Saito, H. Tsutsui, H. Nambu, M. Anada, S. Hashimoto, *Adv. Synth. Catal.* **2005**, *347*, 1483–1487.
[81] T. Takahashi, H. Tsutsui, M. Tamura, S. Kitagaki, M. Nakajima, S. Hashimoto, *Chem. Commun.* **2001**, 1604–1605.
[82] R. Sambasivan, Z. T. Ball, *J. Am. Chem. Soc.* **2010**, *132*, 9289–9291.
[83] R. Sambasivan, Z. T. Ball, *Angew. Chem. Int. Ed.* **2012**, *51*, 8568–8572.
[84] S. K. Baloch, L. Ma, X.-L. Wang, J. Shi, Y. Zhu, F.-Y. Wu, Y.-J. Pang, G.-H. Lu, J.-L. Qi, X.-M. Wang, H.-W. Gu, Y.-H. Yang, *RSC Adv.* **2015**, *5*, 31759–31767.
[85] S. A. Boer, D. R. Turner, *Crystal Growth & Design* **2016**, *16*, 6294–6303; Design **2016**, 16, 6294–6303.
[86] M. Ramesh, P. Makam, C. Voshavar, H. Khare, K. Rajasekhar, S. Ramakumar, T. Govindaraju, *Org. Biomol. Chem.* **2018**, *16*, 7682–7692.
[87] X. Yao, T. Wang, Z. Zhang, *Eur. J. Org. Chem.* **2018**, *2018*, 4475–4478.

Manuscript received: May 28, 2020
Revised manuscript received: July 22, 2020
Accepted manuscript online: July 28, 2020